

Supplementary Material for On-device Adversarial Purification via Distilled and Finetuned Denoising Diffusion Implicit Models

BMVC 2025 Submission # 975

Abstract

This supplementary document provides comprehensive implementation details for the denoising diffusion models central to our work on 'On-device Adversarial Purification via Distilled and Finetuned Denoising Diffusion Implicit Models.' It elaborates on the U-Net architectures for both teacher and distilled student models, their respective diffusion process parameters , and the full training configurations. This includes specifics for the teacher models, the knowledge distillation phase, the finetuning of student models, and the training of downstream classifiers. These details pertain to experiments conducted on the CIFAR-10 and CelebA-HQ datasets, aiming to ensure reproducibility and offer a thorough understanding of our experimental setup.

1 Diffusion Model Setup

Our diffusion models leverage the Denoising Diffusion Probabilistic Model (DDPM) framework [1]. The core denoising network is a U-Net [2], which has been adapted to predict the noise component ε at a given timestep t . Time embeddings, generated through sinusoidal positional encodings that are subsequently projected through linear layers, are integrated into the U-Net's residual blocks. All models were trained using the Adam optimizer with a Mean Squared Error (MSE) loss criterion, measuring the difference between the predicted and true noise. To enhance the quality of generated samples, an Exponential Moving Average (EMA) of the model weights was employed during training.

For the CIFAR-10 dataset, which consists of 32×32 pixel images, the U-Net architecture was configured to process 3-channel (RGB) images. It started with 128 base hidden channels and employed channel multipliers of $[1, 2, 2, 2]$, resulting in 128, 256, 256, and 256 channels at its four respective resolution levels. Each of these levels contained two residual blocks, each incorporating Group Normalization, SiLU activation, and convolutional layers. Time embeddings were added after the first convolution within these blocks. A self-attention mechanism was applied at the second resolution level, corresponding to a 16×16 feature map, and a dropout rate of 0.1 was used. The diffusion process for CIFAR-10 operated over $T = 1000$ timesteps, following a linear beta schedule with $\beta_{\text{start}} = 0.0001$ and $\beta_{\text{end}} = 0.02$. The reverse process variance $q(x_{t-1}|x_t, x_0)$ is β_t . The model was trained to predict the noise

ϵ . Training was conducted using the Adam optimizer with a learning rate of 2×10^{-4} and a batch size of 128 for a total of 2040 epochs. A learning rate warmup period of 5000 steps was utilized, along with gradient clipping at a norm of 1.0. The EMA decay for model weights was set to 0.9999.

For the higher-resolution CelebA-HQ dataset (256×256 images), the U-Net architecture also processed 3-channel (RGB) images, beginning with 128 base hidden channels. The channel multipliers were $[1, 1, 2, 2, 4, 4]$, yielding 128, 128, 256, 256, 512, and 512 channels across six resolution levels. Similar to the CIFAR-10 setup, each level featured two residual blocks with a comparable internal structure. Self-attention was applied at the fifth resolution level (a 16×16 feature map), and a dropout rate of 0.0 was used for this model. The diffusion process for CelebA-HQ also spanned $T = 1000$ timesteps with a linear beta schedule from $\beta_{\text{start}} = 0.0001$ to $\beta_{\text{end}} = 0.02$. However, the reverse process variance $q(x_{t-1}|x_t, x_0)$ is defined as $\tilde{\beta}_t = \frac{1 - \bar{\alpha}_{t-1}}{1 - \bar{\alpha}_t} \beta_t$, with $\bar{\alpha}_t = \prod_{i=1}^t (1 - \beta_i)$. This model also predicted the noise component ϵ . The training utilized the Adam optimizer with a learning rate of 2×10^{-5} and a batch size of 64, running for 1200 epochs. A 5000-step learning rate warmup was included, along with gradient clipping at a norm of 1.0 and an EMA decay of 0.9999.

2 Knowledge Distillation

Knowledge distillation was employed to transfer the denoising capabilities from the larger, pre-trained U-Net teacher models, detailed in Section 1, to more compact student models. This strategy aims to reduce the computational footprint and inference latency, making them suitable for on-device adversarial purification while striving to preserve efficacy. During the distillation process, the teacher model weights were frozen.

For the CIFAR-10 student U-Net (32×32 images), the architecture was a 3-channel (RGB) U-Net with 64 base hidden channels, reduced from the teacher's 128. It used channel multipliers of $[1, 2, 2]$ (compared to the teacher's $[1, 2, 2, 2]$), resulting in 64, 128, and 128 channels across three resolution levels. Each level contained one residual block, a reduction from the teacher's two, while retaining Group Normalization, SiLU activation, convolutional layers, and time embedding integration. Self-attention was applied at the second resolution (16×16 feature map), and a dropout rate of 0.1 was maintained.

For the CelebA-HQ student U-Net (256×256 images), the architecture was also a 3-channel (RGB) U-Net, but with 96 base hidden channels (teacher: 128). It employed channel multipliers of $[1, 1, 2, 2, 3]$ across five resolution levels (teacher: $[1, 1, 2, 2, 4, 4]$ over six levels). Each level comprised one residual block (teacher: 2), while retaining the core components. Self-attention was applied at the fourth resolution level (a 32×32 feature map). The dropout rate was set to 0.05 (teacher: 0.0).

Regarding distillation training, the Adam optimizer was used with an initial learning rate of 2×10^{-4} , which included a linear warmup phase over 5000 steps. Training proceeded for 500 epochs. Gradients were clipped to an L_2 norm of 1.0. An EMA of student weights with a decay of 0.9999 was maintained. Specifically, the CIFAR-10 student model was trained with a batch size of 2048, while the CelebA-HQ student model used a batch size of 32.

2.1 Finetuning

After the knowledge distillation phase, the compact student models were further finetuned on their respective datasets (CIFAR-10 and CelebA-HQ) to potentially enhance their per-

092 formance. The finetuning process continued to use the DDPM objective, where the model
093 predicts the noise component ϵ added to an image at a given timestep t , optimized using a
094 MSE loss. For both datasets, the student models were finetuned using the Adam optimizer
095 with a learning rate of 1×10^{-5} for 100 epochs. A linear learning rate warmup was applied
096 over the first 500 training steps. Similar to the distillation training, gradients were clipped
097 to an L_2 norm of 1.0, and an Exponential Moving Average (EMA) of the model weights
098 was maintained with a decay of 0.9999. The batch size during finetuning was set to 128 for
099 the CIFAR-10 student model and 32 for the CelebA-HQ student model. The U-Net archi-
100 tectures of the student models and the diffusion process parameters (beta schedule, $T=1000$
101 timesteps) remained unchanged from their configuration in the distillation stage.

102

103 3 Classifiers

104

105 For the classification, we trained a WideResNet-28-10 for CIFAR-10 and a ResNet-18 for
106 CelebA-HQ.

107 The WideResNet-28-10 for CIFAR-10 was trained using the Stochastic Gradient De-
108 scent (SGD) optimizer. The optimizer was configured with an initial learning rate of 0.2, a
109 momentum of 0.9, weight decay of 5e-4. A MultiStepLR scheduler was used to reduce the
110 learning rate by a factor of 0.2 at epochs 60, 120, and 160. The training loop ran for a maxi-
111 mum of 200 epochs with a batch size of 512, utilizing Cross-Entropy Loss. The architecture
112 itself incorporated a dropout rate of 0.3. For data handling and setup, 10% of the CIFAR-10
113 training data (5000 images) was reserved for validation.

114 For ResNet-18 on CelebA-HQ, the model was trained using the AdamW optimizer. This
115 optimizer was set up with an initial learning rate of 0.008 and a weight decay of 0.01. A
116 CosineAnnealingLR scheduler adjusted the learning rate, with T_{\max} set to 50 epochs and
117 η_{\min} to 1% of the initial learning rate. The training loop proceeded for a maximum of 50
118 epochs, using a batch size of 1024 and Cross-Entropy Loss. Input images were resized to
119 256x256. During training, data augmentation consisted of random horizontal flips.

120

121 4 Qualitative Examples

122

123 This section presents qualitative results of our adversarial purification methods on both
124 CIFAR-10 and CelebA-HQ datasets. Figure 1 & 2 below illustrate the visual quality of
125 images after being subjected to adversarial attacks and subsequently purified by DDPM, our
126 standard DDIM approach, and our distilled finetuned DDIM variant.

127

128 References

129

- 130 [1] Jonathan Ho, Ajay Jain, and Pieter Abbeel. Denoising diffusion probabilistic models.
131 *Advances in neural information processing systems*, 33:6840–6851, 2020.
- 132
- 133 [2] Olaf Ronneberger, Philipp Fischer, and Thomas Brox. U-net: Convolutional networks
134 for biomedical image segmentation. In Nassir Navab, Joachim Hornegger, William M.
135 Wells, and Alejandro F. Frangi, editors, *Medical Image Computing and Computer-
136 Assisted Intervention – MICCAI 2015*, pages 234–241, Cham, 2015. Springer Interna-
137 tional Publishing. ISBN 978-3-319-24574-4.

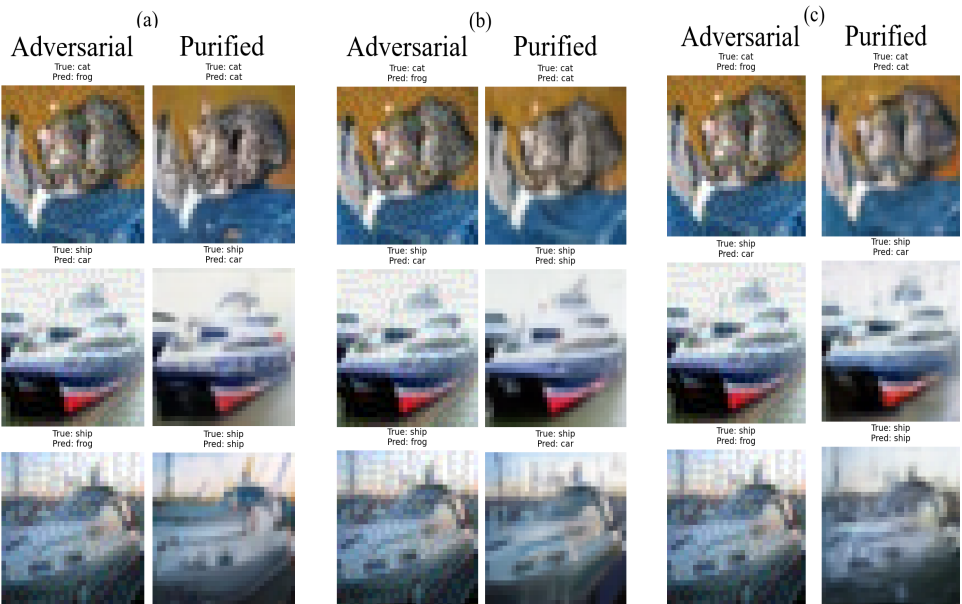


Figure 1: Qualitative examples of adversarial purification on the CIFAR-10 dataset against FGSM_{L_∞} (8/255). The figure shows results from three methods: (a) DDPM Purification, (b) DDIM Purification, and (c) Distilled Finetuned DDIM Purification. Each panel (a, b, c) displays multiple image examples (rows), with columns showing the adversarially attacked image (left), and the purified image (right). The initial noising timestep for all purification methods is $t^* = 0.075$. For DDIM-based methods (b and c), the number of reverse steps is $S_{DDIM} = 30$.

138
139
140
141
142
143
144
145
146
147
148
149
150
151
152
153
154
155
156
157
158
159
160
161
162
163
164
165
166
167
168
169
170
171
172
173
174
175
176
177
178
179
180
181
182
183

184

185

186

187

188

189

190

191

192

193

194

195

196

197

198

199

200

201

202

203

204

205

206

207

208

209

210

211

212

213

214

215

216

217

218

219

220

221

222

223

224

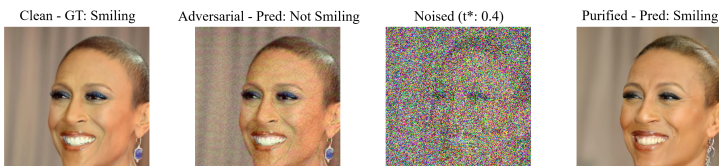
225

226

227

228

229



(a) DDPM Purification

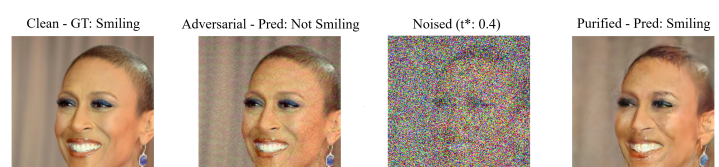
(b) DDIM Purification ($S_{DDIM} = 30$)(c) Distilled Finetuned DDIM Purification ($S_{DDIM} = 30$)

Figure 2: Purification examples on the CelebA-HQ dataset against FGSM_{L_∞} (8/255). (a) DDPM Purification. (b) DDIM Purification. (c) Distilled Finetuned DDIM Purification. Each panel displays two examples (stacked vertically), showing the original image (left), attacked image (center), and purified image (right). For all purification methods, the initial noising timestep is $t^* = 0.4$. For DDIM-based methods (b and c), $S_{DDIM} = 30$.